J. Fluid Mech. (1987), *vol.* 179, *pp.* 253–266
Printed in Great Britain

The damping of capillary–gravity waves at a rigid boundary

By L. M. HOCKING

Department of Mathematics, University College London, Gower Street, London WC1E 6BT, UK

(Received 9 July 1985 and in revised form 10 October 1986)

The frequency and damping rate of surface capillary–gravity waves in a bounded region depend on the conditions imposed where the free surface makes contact with the boundary. Extreme cases are when the free surface meets the boundary orthogonally, as in the case of pure gravity waves, and when the contact line remains fixed throughout the motion. An edge condition that models to some extent the dynamics associated with moving contact lines, but not contact-angle hysteresis, is given by making the slope of the free surface at contact proportional to its velocity. This model, which includes the two extreme cases, is used to obtain the frequency and damping rate of a standing wave between two parallel vertical walls. The effect of viscosity in the boundary layers on the walls is included and it is shown that the dissipation associated with the surface forces can exceed that produced by viscosity. The results are compared with those obtained from a number of experimental investigations, in which damping rates too large to be attributed to viscous action have been measured.

1. Introduction

Most research on capillary–gravity waves on a free liquid surface has concentrated on their propagation. In a confined region, the methods for determining the frequencies of standing gravity waves are well known (Lamb 1932 chapter 9), at least for vertical boundaries. In large basins, like harbours and lakes, capillarity can safely be ignored, but this is not so when the container has a horizontal dimension of typically a few centimetres. Even then, the effect of capillarity does not introduce more than a quantitative change except for very small containers, high-frequency modes and low-gravity environments.

The presence of capillarity adds an extra term to the free-surface pressure condition. This term is proportional to the curvature of the free surface and, for progressive waves, produces a change in the frequency of the waves for given wavenumber. The increase in the order of the pressure condition, however, requires extra conditions to be imposed when the solution is sought in a finite region. These conditions control the position of the free surface at its intersection with the boundary of the container.

Without capillarity, the free surface must intersect the vertical walls orthogonally. If this is imposed as the required condition when capillarity is present, the only influence of this extra feature is to alter the frequency of the standing waves in the container in a similar way to the change produced in progressive waves. But it is far from clear that the condition of orthogonal intersection of free surface and boundary is the appropriate one for standing capillary–gravity waves.

Recent work by Benjamin & Scott (1979) and Graham-Eagle (1983, 1984) has examined an alternative boundary condition at the edge of the free surface, namely that in which the surface elevation there is unchanged from its equilibrium position. These authors argue that this is the appropriate condition for a rim-full container and calculate the frequencies for progressive waves along a channel with sidewalls, two-dimensional standing waves between two vertical boundaries and standing waves in a circular cylinder. The change in the edge condition makes such problems considerably more difficult. With orthogonal intersection, the fluid motion and the elevation of the free surface can be found in terms of a single separated-variable mode for each frequency. With zero elevation at the edge, the complete set of such modes of the fluid motion must be used and the frequencies are given by the zeros of a function defined by an infinite series, all the terms of which depend on the frequency.

Benjamin & Scott (1979) argue that the pinned-end edge condition may also be appropriate when the container is not rim-full. When a fluid interface and a solid boundary intersect, the Young–Laplace equation shows that the angle of intersection is fixed in static conditions. A large body of experimental evidence (see Dussan V. 1979) indicates that such a unique contact angle does not exist in general. If by the contact angle is meant the angle as measured at some small distance from the actual contact line, removed from the immediate influence of molecular effects and surface roughnesses, a range of static angles appears to exist, centred on the Young–Laplace angle, within which equilibrium can be maintained. This range is exceeded when the contact line moves, the angle increasing when the interface moves forward, that is, in the direction away from the bulk of the fluid. When the interface moves in the opposite direction, the contact angle is reduced to values less than the minimum of the static range.

The extension of the gravity-wave condition of an orthogonal intersection, the *free-end* edge condition, to waves with capillarity implies that the contact angle is fixed at 90° with no dynamic behaviour and that the contact line can move freely across the solid boundary. Benjamin & Scott (1979) suggest that if the Young–Laplace angle is 90° and the wave is of small amplitude, then the slope at the wall will lie within the static range of contact angle and the edge condition should be replaced by one in which the edge remains stationary, the *pinned-end* edge condition. If the Young–Laplace angle is not 90°, the equilibrium position of the free surface is not flat and the determination of the standing-wave frequencies becomes much more difficult whatever edge condition is applied. When the waves have small amplitude, the free-surface conditions can be applied at the undisturbed position of the surface and the solution is more difficult to obtain when this surface is not flat. Apart from some general results relating to this situation by Graham-Eagle (1984), I know of no published work on this problem.

The range of possible static contact angles appears to be related to surface roughnesses on the solid boundary (Jansons 1985) and can be reduced by careful preparation of the material. It is possible, therefore, that the wave amplitude may be sufficiently large (but still small enough for linear theory to be adequate) that the static range of contact angle is exceeded, and the dynamic behaviour then becomes significant. To allow for both the static range and the dynamic behaviour in the edge condition would require the imposed boundary condition to change its form during the motion and would be difficult to implement. A more profitable alternative, suggested by Davis (1980) in a different context, is to explore the situation when the static range of angle is negligibly small, in which case the dynamic behaviour becomes the significant feature. If the static angle is again taken to be 90° and a linear variation

of contact angle with the speed of the contact line is taken to be sufficiently accurate, the edge condition has the form

$$\frac{\partial \eta'}{\partial t'} = \lambda' \frac{\partial \eta'}{\partial n}, \tag{1}$$

where η' is the free-surface elevation, t' is the time, n is normal to the solid boundary drawn into the fluid and λ' is some constant, measuring the ratio of the speed of the contact line to the change in contact angle. This condition takes into account some of the wetting properties of the fluid and will be referred to as the *wetting* condition. The assumed linearity is probably sufficiently accurate unless the amplitude of the waves, and hence the speed of the contact line, is so large that the dynamic angle approaches its limiting values of 0° or 180°. An important feature of this condition is that it includes, as special cases, both the free-end ($\lambda' = \infty$) and the pinned-end ($\lambda' = 0$) edge conditions.

There are two questions of major importance in studying standing waves. One is the determination of their possible frequencies and the other is their damping rate. The damping of gravity waves was examined theoretically by Ursell (1952), who showed that the major contribution came from the action of viscosity at the sidewalls, except for very wide or very shallow containers. Miles (1967) studied the damping in closed basins, including the effects of capillary hysteresis. He assumed that the contact angle takes constant but different values, depending on the direction of motion of the contact line and deduced the dissipation from the rate of working of the capillary forces. The fraction of the time period during which the contact angle changes and the contact line is at rest is ignored. The frequency of the wave is determined without reference to the edge conditions, that is, the free-end value is tacitly assumed.

The importance of the edge region in the calculation of the viscous damping of surface waves has been demonstrated by Mei & Liu (1973). They show that the Stokes layer at the wall interacts with the free surface in a corner region which acts as an oscillating source and forces an interior potential flow of order $\nu^{\frac{1}{2}}$, where ν is the kinematic viscosity. It is essential that this contribution be included when calculating the leading-order term in the viscous damping rate. The forced pressure has a logarithmic singularity at the corner, as expected when a moving contact line is present. In the absence of surface tension, as in the analysis of Mei & Liu, the surface elevation is also unbounded at the edge. When surface tension is present, however, the singular pressure is balanced by the free-surface curvature, and the elevation is uniformly small.

Measurements of the damping of surface waves have been made by Benjamin & Ursell (1954), Case & Parkinson (1957) and Keulegan (1959) for containers of various shapes. The degree of agreement between these observations and the predicted values of the damping rate based on the action of viscosity is variable and seems to depend on the properties of the particular materials used and the preparation of the solid boundaries. One suggestion made by these authors is that the discrepancy between theory and observation may result from the neglected capillary effects, particularly when associated with the behaviour of the interface near the edge, but I am not aware of any attempt to carry out their proposals for further study, apart from the paper by Miles (1967). It should, however, be emphasized that a major contributor to the excessive damping rates is likely to be contamination by surface-active agents.

The change from the free-end edge condition used by these authors to the pinned-end condition suggested by Benjamin & Scott (1979) is not likely to lead to

an improvement in the gap between theory and experiment. The damping rate when this edge condition is used is probably less than that for the free-end condition because of the reduction in the movement of the interface at the contact line and hence of the fluid near to it. The discrepancy, however, is in the opposite direction, the observed damping rates being often considerably greater than the theoretical predictions. The wetting boundary condition, on the other hand, implies the dissipation of energy at the contact line and this new contribution to the decay rate of the waves may be equal to or greater than that produced by viscosity.

Except when $\lambda' = 0$, the wetting edge condition implies a moving contact line. It is well known that viscous stresses become singular at such a line and in order to obtain bounded dissipation rates it is necessary to resolve this singularity. One way by which this can be achieved is by postulating a small slip region near the contact line (see Dussan V. 1979). Whatever the nature of the slip and the detailed structure of the flow in this region, the macroscopic effect is to replace the unbounded dissipation of energy at the contact line by a value proportional to the viscosity and to the logarithm of the scaled extent of the slip region. In the present work, the dissipation is only calculated to first order in a small parameter proportional to the square root of the viscosity so that the contribution to the dissipation from the neighbourhood of the contact line only enters at a later stage in the expansion. It is therefore possible to ignore the effect of the moving contact line; however, it is possible that the value of the parameter λ' in the wetting edge condition may be partly dependent on what is happening in the contact line region.

In this paper the wetting condition is applied to the problem of standing capillary–gravity waves between two parallel vertical walls. The frequencies of these waves, and their damping both by wetting and by viscosity, are calculated. Since the value of the coefficient λ' in the wetting condition is not precisely known, there is little point, in this exploratory study, in finding solutions for the particular geometries relevant to the experiments mentioned before, although there is no difficulty, in principle, in carrying out these calculations. Some measure of the likely effect of the wetting condition in producing dissipation of the waves can be deduced from the particular and simple cases studied. These estimates are compared in the final section of this paper with the observations of Benjamin & Ursell (1954), Case & Parkinson (1957) and Keulegan (1959). In some cases it appears that the proposed wetting condition predicts decay rates as large as those observed, but in others the discrepancy between theory and observation cannot be explained in this way.

Before proceeding with the details of the solution, it is perhaps advisable to list the assumptions on which the theory is based. The static contact angle is 90°, the waves are two-dimensional and of small amplitude, the boundaries are vertical and the depth of the fluid is sufficiently large compared with the wavelength and the width of the container for the bottom to have a negligible effect. The use of the wetting condition implies that the smallest lengthscales used are large compared to the microscopic scales relevant to the immediate vicinity of the contact line, namely the molecular scale and the size of the roughnesses on the solid wall. The smallest lengthscale occurring in the solution is the thickness of the viscous boundary layer at the wall, typically 1 mm, whereas the maximum lengthscale associated with surface roughness is usually less than 1 μm.

2. Two-dimensional standing waves

If fluid is confined between two parallel vertical walls, standing waves with crests parallel to the walls can be generated. Let (x, y) (a/π) be Cartesian coordinates with

origin in the equilibrium free surface midway between the walls. The x-axis is normal to the walls, the y-axis is in the upward vertical direction, and the distance between the walls is a. The velocity components are (u, v) $(ag/\pi)^{\frac{1}{2}}$ and the time is $t(a/\pi g)^{\frac{1}{2}}$, where g is the gravitational acceleration. There is no variation in the horizontal direction parallel to the walls. The linearized equations of fluid motion are:

$$\frac{\partial u}{\partial t} = -\frac{\partial p}{\partial x} + f\frac{\partial^2 u}{\partial x^2}, \tag{2}$$

$$\frac{\partial v}{\partial t} = -\frac{\partial p}{\partial y} + f\frac{\partial^2 v}{\partial x^2}, \tag{3}$$

$$\frac{\partial u}{\partial x} + \frac{\partial v}{\partial y} = 0, \tag{4}$$

where p is the non-dimensional pressure, f is an inverse Reynolds number, and only the relevant viscous terms are included. Viscosity is most important in the boundary layer at the wall and its effect in the body of the fluid and at the free surface are ignored.

The boundary conditions are that the velocities tend to zero as $y \to -\infty$ and that there is no slip at the walls, so that

$$u = 0, \quad v = 0 \quad \text{at } x = \pm\tfrac{1}{2}\pi. \tag{5}$$

If $\eta(x, t)$ is the free-surface elevation above its equilibrium position $y = 0$, the kinematic and pressure conditions there, in linearized form, are

$$\frac{\partial \eta}{\partial t} = v, \tag{6}$$

$$\eta - K\frac{\partial^2 \eta}{\partial x^2} = p, \tag{7}$$

where K is the capillarity coefficient. Finally, the wetting edge condition proposed in the previous section is

$$\frac{\partial \eta}{\partial t} \pm \lambda \frac{\partial \eta}{\partial x} = 0 \quad \text{at } x = \pm\tfrac{1}{2}\pi, \tag{8}$$

where λ is the non-dimensional form of the coefficient λ' in (1). The solution of these equations depends on the values of three parameters,

$$\lambda = \lambda'\left(\frac{\pi}{ag}\right)^{\frac{1}{2}}, \quad f = \nu\left(\frac{\pi^3}{a^3 g}\right)^{\frac{1}{2}}, \quad K = \frac{\pi^2 \gamma}{\rho g a^2}, \tag{9}$$

where ρ, ν, γ are respectively the density, kinematic viscosity and surface tension of the fluid. The viscosity parameter f is assumed to be small, whereas the wetting parameter λ and the capillarity parameter K can have all values from zero to infinity.

The waves can be divided into two classes, the odd modes in which p, v and η are odd in x and u is even, and the even modes which have the opposite parity. The first class will be analysed in detail and only a summary of the corresponding results for the even modes will be given. It is expected that the mode with lowest frequency is an odd mode; this is certainly the case when the free-end edge condition is used. The solution (to the order studied) can be split into three parts: the $O(1)$-motion in the interior of the fluid, boundary-layer solutions near each wall, and the $O(f^{\frac{1}{2}})$-motion in the interior forced by these boundary layers and the corner regions. There is no

forcing of the solution at a given frequency and the goal of the analysis is the determination of the complex frequency to $O(f^{\frac{1}{2}})$, the (positive) imaginary part giving the damping rate.

The fluid motion in the interior for the odd modes can be written in the form

$$p_0 = \sigma \sum_{n=0}^{\infty} P_n \sin(2n+1)x\, e^{(2n+1)y}, \tag{10}$$

$$u_0 = i \sum_{n=0}^{\infty} (2n+1) P_n \cos(2n+1)x\, e^{(2n+1)y}, \tag{11}$$

$$v_0 = i \sum_{n=0}^{\infty} (2n+1) P_n \sin(2n+1)x\, e^{(2n+1)y}; \tag{12}$$

a time factor $\exp(i\sigma t)$ has been dropped from each term.

This form of the solution satisfies the equations with $f = 0$, the boundary conditions of no normal velocity at the walls and the condition at $y = -\infty$. The slip velocity parallel to the wall can be reduced to zero by the addition of the solutions

$$u_{\pm} = -i\omega\left(\sum_{n=0}^{\infty} (-1)^n (2n+1)^2 P_n e^{(2n+1)y}\right) \exp\left\{\frac{(\frac{1}{2}\pi \mp x)}{\omega}\right\}, \tag{13}$$

$$v_{\pm} = \mp i\left(\sum_{n=0}^{\infty} (-1)^n (2n+1) P_n e^{(2n+1)y}\right) \exp\left\{\frac{(\frac{1}{2}\pi \mp x)}{\omega}\right\}, \tag{14}$$

in the boundary layers at $x = \pm\frac{1}{2}\pi$, where

$$\omega = \frac{f^{\frac{1}{2}} e^{\frac{3}{4}\pi i}}{\sigma^{\frac{1}{2}}}.$$

These values of u_+ and u_- do not vanish at the appropriate walls, so there must be a correction of $O(f^{\frac{1}{2}})$ to the interior motion. This correction can be written in terms of a pressure p_1, where

$$\nabla^2 p_1 \equiv \frac{\partial^2 p_1}{\partial x^2} + \frac{\partial^2 p_1}{\partial y^2} = 0, \tag{15}$$

and

$$\frac{\partial p_1}{\partial x} = \omega\sigma \sum_{n=0}^{\infty} (-1)^n (2n+1)^2 P_n e^{(2n+1)y} \quad \text{at } x = \pm\tfrac{1}{2}\pi. \tag{16}$$

The free-surface conditions (6) and (7) have the forms

$$\sigma^2\eta = \frac{\partial p}{\partial y} + B(x), \tag{17}$$

$$\eta - K\frac{\partial^2 \eta}{\partial x^2} = p, \tag{18}$$

which are to be evaluated at $y = 0$. The boundary-layer contribution, $B(x)$, is defined by

$$B(x) = -\sigma\left(\sum_{n=0}^{\infty} (-1)^n (2n+1) P_n\right)\left(\exp\left\{\frac{\frac{1}{2}\pi - x}{\omega}\right\} - \exp\left\{\frac{\frac{1}{2}\pi + x}{\omega}\right\}\right). \tag{19}$$

If we now expand both η and σ in the form

$$\eta = \eta_0 + \eta_1 + \ldots, \quad \sigma = \sigma_0 + \sigma_1 + \ldots, \tag{20}$$

the first two terms in (17) and (18) are

$$\sigma_0^2\eta_0 = \frac{\partial p_0}{\partial y}, \quad \sigma_0^2\eta_1 + 2\sigma_0\sigma_1\eta_0 = \frac{\partial p_1}{\partial y} + B(x), \tag{21a,b}$$

$$\eta_0 - K\frac{\partial^2\eta_0}{\partial x^2} = p_0, \quad \eta_1 - K\frac{\partial^2\eta_1}{\partial x^2} = p_1, \tag{22a,b}$$

all of which are to be evaluated at $y = 0$. The value of η_0, determined by (10) and (21a) is given by

$$\eta_0 = \frac{1}{\sigma_0}\sum_{n=0}^{\infty}(2n+1)\,P_n \sin(2n+1)\,x, \tag{23}$$

and then (22a) becomes

$$K\frac{\partial^2\eta_0}{\partial x^2} = \frac{1}{\sigma_0}\sum_{n=0}^{\infty}(2n+1-\sigma_0^2)\,P_n \sin(2n+1)\,x. \tag{24}$$

The solution of this equation is

$$\eta_0 = \sum_{n=0}^{\infty}\frac{\sigma_0^2-2n-1}{\sigma_0 K(2n+1)^2}P_n \sin(2n+1)\,x + Ax, \tag{25}$$

where A is a constant. If we express Ax as a Fourier sine series and equate the values of η_0 given by (23) and (25), we obtain

$$P_n = -\frac{4AK\sigma_0(-1)^n}{\pi d_{2n+1}(\sigma_0)}, \tag{26}$$

where

$$d_n(\sigma) = \sigma^2 - n - Kn^3. \tag{27}$$

The edge conditions (8), to leading order, imply that

$$\mathrm{i}\sum_{n=0}^{\infty}(-1)^n(2n+1)\,P_n + \lambda A = 0, \tag{28}$$

and it follows from (26) that the equation for the frequency σ_0 is

$$\sum_{n=0}^{\infty}\frac{2n+1}{d_{2n+1}(\sigma_0)} + \frac{\mathrm{i}\pi\lambda}{4K\sigma_0} = 0. \tag{29}$$

The analysis leading to this equation for the frequency is similar to that given by Benjamin & Scott (1979) for the special case $\lambda = 0$. The free-end edge condition is $\lambda = \infty$, and (29) can only be satisfied if a term in the infinite series has a zero denominator. This gives the familiar result

$$\sigma_0^2 = 2n+1+K(2n+1)^3. \tag{30}$$

In both the free- and the pinned-end cases, the values of σ_0 are real. For general values of λ, it is clear from (70) that σ_0 has an imaginary part and the wetting edge condition involves dissipation of energy, which leads to a damping of the waves.

In order to determine the correction of order $f^{\frac{1}{2}}$ to the complex frequency, it is not necessary to determine p_1, η_1 and the associated velocity components. The method of Mei & Liu (1973) used here determines σ_1 from integrated forms of the equations.

Since both p_0 and p_1 are harmonic functions,

$$\int_{-\infty}^{0}\int_{-\frac{1}{2}\pi}^{\frac{1}{2}\pi}(p_0\nabla^2 p_1 - p_1\nabla^2 p_0)\,\mathrm{d}x\,\mathrm{d}y = 0. \tag{31}$$

The divergence theorem can be used to express this integral in terms of integrals over the boundary of the fluid and we obtain

$$\int_{-\infty}^{0}\left[p_0\frac{\partial p_1}{\partial x}-p_1\frac{\partial p_0}{\partial x}\right]_{-\frac{1}{2}\pi}^{\frac{1}{2}\pi}\mathrm{d}y+\int_{-\frac{1}{2}\pi}^{\frac{1}{2}\pi}\left[p_0\frac{\partial p_1}{\partial y}-p_1\frac{\partial p_0}{\partial y}\right]_{-\infty}^{0}\mathrm{d}x=0. \tag{32}$$

Since $\partial p_0/\partial x = 0$ at $x = \pm\frac{1}{2}\pi$ the values of p_1 there are not needed, and $\partial p_1/\partial x$ is given by (16). The values of p_1 and $\partial p_1/\partial x$ at the free surface can be found from (21*b*) and (22*b*). Hence the remaining unknown, σ_1, can be determined. On making use of the known value of p_0 and the equation satisfied by σ_0, and after integration by parts, the evaluation of (32) finally leads to the following equation for the frequency correction σ_1:

$$\sigma_1=\frac{2}{\pi}\mathrm{e}^{\frac{3}{4}\pi\mathrm{i}}f^{\frac{1}{2}}\sigma_0^{\frac{1}{4}}\frac{\displaystyle\int_{-\infty}^{0}\left(\sum_{n=0}^{\infty}\frac{(2n+1)\,\mathrm{e}^{(2n+1)y}}{d_{2n+1}(\sigma_0)}\right)^2\mathrm{d}y}{\displaystyle\sum_{n=0}^{\infty}\frac{2n+1}{d_{2n+1}^2(\sigma_0)}+\frac{\mathrm{i}\pi\lambda}{8K\sigma_0^3}}. \tag{33}$$

The complex frequency to the order calculated is given by $\sigma = \sigma_0+\sigma_1$. The real parts of σ_0 and σ_1 determine the frequency of the wave and the viscous correction to leading order. The imaginary parts give the damping rates produced by the wetting condition and viscosity, respectively.

For the even modes the interior solution has the form

$$p_0=\mathrm{e}^{\mathrm{i}\sigma t}\left\{\sum_{n=1}^{\infty}P_n\cos 2nx\,\mathrm{e}^{2ny}+P_0\right\}. \tag{34}$$

The presence of the spatially constant pressure term P_0 is a novel feature of the even modes and it can be determined by requiring that the volume of the fluid remain constant, which is equivalent to the condition

$$\int_{-\frac{1}{2}\pi}^{\frac{1}{2}\pi}\eta\,\mathrm{d}x=0. \tag{35}$$

In the odd modes, this condition is automatically satisfied and the constant pressure term is excluded, since the pressure is an odd function of x in these modes. Similar analysis to that described in connection with the odd modes leads to equations for the leading terms in the frequency of the form

$$\sum_{n=1}^{\infty}\frac{2n}{d_{2n}(\sigma_0)}+\frac{\mathrm{i}\pi\lambda}{4K\sigma_0}=0, \tag{36}$$

$$\sigma_1=\frac{2}{\pi}\mathrm{e}^{\frac{3}{4}\pi\mathrm{i}}f^{\frac{1}{2}}\sigma_0^{\frac{1}{4}}\frac{\displaystyle\int_{-\infty}^{0}\left(\sum_{n=1}^{\infty}\frac{2n\,\mathrm{e}^{2ny}}{d_{2n}(\sigma_0)}\right)^2\mathrm{d}y}{\displaystyle\sum_{n=1}^{\infty}\frac{2n}{d_{2n}^2(\sigma_0)}+\frac{\mathrm{i}\pi\lambda}{8K\sigma_0^3}}. \tag{37}$$

For both classes of modes, the evaluation of the frequencies is a numerical task. When $\lambda = 0$, it is clear that real values of σ_0 exist between successive zeros of the denominators in (29) and (36). These values can be found first, for a particular value of K, and used as starting values in the search for solutions as λ is increased. Complex Newton–Raphson iteration enabled the roots to be found quickly, although some care was necessary in the choice of an initial guess in the iteration to prevent the process jumping back to a previously determined root. There are an infinite number of roots

	λ							
K	0	0.1	1	2	5	10	100	∞
0	1	1	1	1	1	1	1	1
	0	0	0	0	0	0	0	0
0.1	1.2833	1.2688	1.0617	1.0520	1.0493	1.0489	1.0488	1.0488
	0	0.0650	0.0621	0.0317	0.0127	0.0064	0.0006	0
1	2.4564	2.4518	1.7421	1.4503	1.4191	1.4154	1.4142	1.4142
	0	0.0971	0.7570	0.3368	0.1284	0.0638	0.0064	0
2	3.2987	3.2955	2.8730	1.8139	1.7401	1.7340	1.7321	1.7321
	0	0.1025	1.0593	0.7424	0.2601	0.1280	0.0127	0
5	5.0417	5.0397	4.8272	3.6964	2.4641	2.4524	2.4495	2.4495
	0	0.1064	1.0919	2.2191	0.6770	0.3229	0.0318	0
10	7.0460	7.0446	6.9053	6.3650	3.3458	3.3200	3.3167	3.3166
	0	0.1078	1.0933	2.2765	1.4668	0.6564	0.0637	0
100	22.0394	22.0388	21.9976	21.8700	20.8412	12.9129	10.0491	10.0499
	0	0.1091	1.0928	2.1956	5.6668	10.9859	0.6386	0

TABLE 1. Real (top) and imaginary (bottom) parts of σ_0

	λ							
K	0	0.1	1	2	5	10	100	∞
0		−0.2251	−0.2251	−0.2251	−0.2251	−0.2251	−0.2251	−0.2251
		0.2251	0.2251	0.2251	0.2251	0.2251	0.2251	0.2251
0.1	−0.1254	−0.0956	−0.2194	−0.2252	−0.2282	−0.2293	−0.2304	−0.2305
	0.1254	0.1665	0.2490	0.2380	0.2331	0.2318	0.2306	0.2305
1	−0.1552	−0.1345	−0.3987	−0.3648	−0.2947	−0.2796	−0.2687	−0.2677
	0.1552	0.1765	0.6554	0.2596	0.2525	0.2586	0.2666	0.2677
2	−0.1784	−0.1606	+0.0244	−0.5709	−0.3557	−0.3217	−0.2985	−0.2962
	0.1784	0.1964	0.5671	0.3084	0.2642	0.2772	0.2940	0.2962
5	−0.2194	−0.2051	−0.0505	−0.0751	−0.5129	−0.4141	−0.3574	−0.3523
	0.2194	0.2337	0.4067	1.3446	0.2831	0.3098	0.3473	0.3523
10	−0.2589	−0.2468	−0.1256	+0.0673	−0.7935	−0.5289	−0.4191	−0.4099
	0.2589	0.2710	0.3952	0.6943	0.3057	0.3377	0.4012	0.4099
100	−0.4572	−0.4503	−0.3880	−0.3142	−0.0275	−1.9467	−0.7701	−0.7135
	0.4572	0.4640	0.5259	0.5992	0.9320	4.4159	0.6642	0.7135

TABLE 2. Real (top) and imaginary (bottom) parts of $f^{-\frac{1}{2}}\sigma_1$

of both classes, the first few of which were calculated for a restricted range of values of λ and K. Most attention, however, was given to the odd mode of lowest frequency. When $\lambda = \infty$, this mode is the fundamental sloshing mode in which there is a single nodal line on the free surface (at $x = 0$).

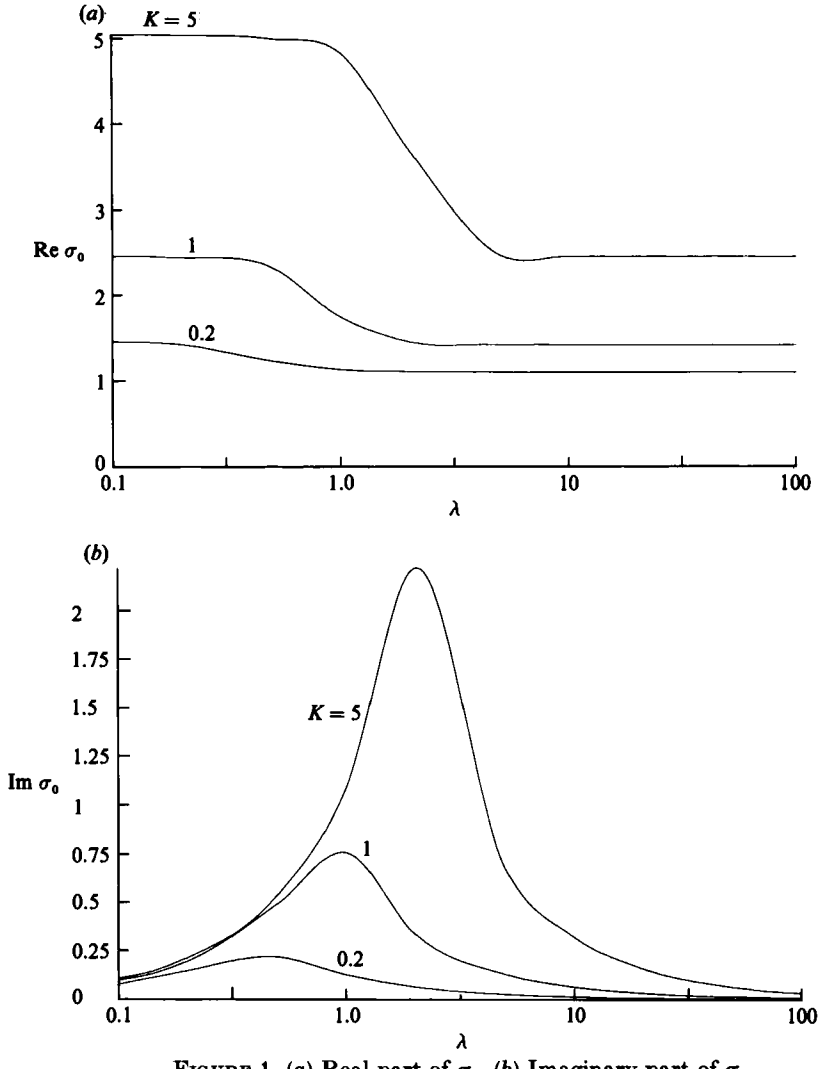

FIGURE 1. (*a*) Real part of σ_0. (*b*) Imaginary part of σ_0.

Some of the results obtained are given in tables 1 and 2 and figures 1 and 2. The entries in table 1 contain the real (top line) and imaginary (bottom line) parts of σ_0 (see also figure 1). The frequency decreases with increasing λ, but the total variation is not large. Even for large K the ratio of the extreme values at $\lambda = 0$ and ∞ is no more than about two. The imaginary parts give the damping rate associated with capillarity and the edge condition. As predicted this is zero for the free- and pinned-end cases, but intermediate values of λ give significant damping rates. The maximum values as a function of λ occur at values of λ proportional to $K^{\frac{1}{2}}$, and they increase with K. In table 2 the entries, when multiplied by $f^{\frac{1}{2}}$, give the viscous correction to the frequency and the viscous damping rate in the top and bottom lines, respectively (see figure 2). The frequency correction has a complicated dependence on both λ and K, but it is not a particularly significant quantity. The viscous damping coefficient has a weak dependence on both λ and K, except for the appearance of narrow peaks where λ is proportional to $K^{\frac{1}{2}}$, where values in excess of 0.6 are obtained.

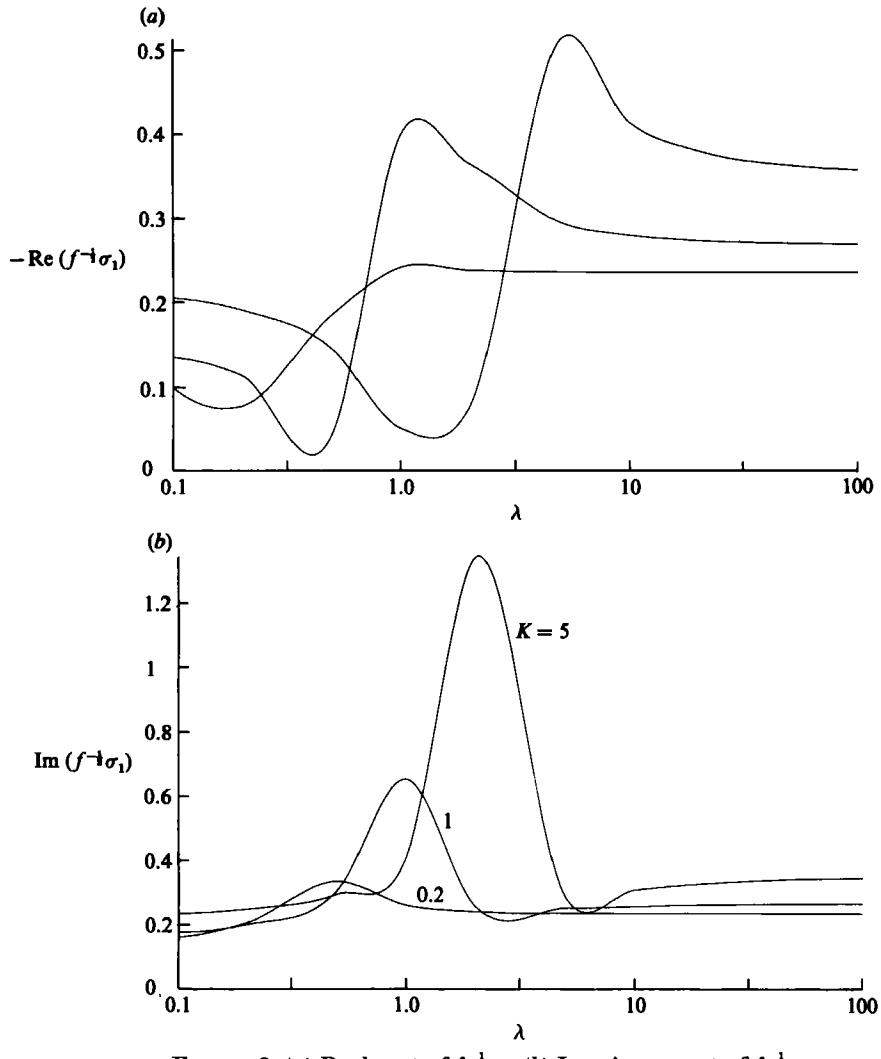

FIGURE 2. (*a*) Real part of $f^{-\frac{1}{3}}\sigma_1$. (*b*) Imaginary part of $f^{-\frac{1}{3}}\sigma_1$.

Some limiting values of σ can be expressed analytically, using the definitions of σ_0 and σ_1 in (29) and (33) and the calculated results. For $\lambda = \infty$, we find that

$$\sigma = (1+K)^{\frac{1}{2}} + \frac{(-1+\mathrm{i})}{\pi\sqrt{2}} f^{\frac{1}{2}}(1+K)^{\frac{1}{4}}. \tag{38}$$

The limits $\lambda = \infty$ and $K = 0$ are equivalent, so that when $K = 0$ we have

$$\sigma = 1 + \frac{(-1+\mathrm{i})}{\pi\sqrt{2}} f^{\frac{1}{2}}. \tag{39}$$

For K large, the dependence of σ on K can be deduced from (29) and (33) and the numerical constants estimated from the calculated results for $K = 100$. In this limit, the value of σ is given approximately by the expression

$$\sigma = 2.2K^{\frac{1}{2}} + 0.11\mathrm{i}\lambda + 0.145(-1+\mathrm{i}) f^{\frac{1}{2}} K^{\frac{1}{4}}. \tag{40}$$

It should be noted that the order in the double limits $\lambda = 0$, $K = 0$ and $\lambda = \infty$, $K = \infty$ is important.

3. Comparison with experimental values

The predicted damping rates for standing waves between two walls enable the relative importance of viscous damping and that produced by capillary action to be assessed. Experiments on the damping of standing waves have been performed in containers of various shapes by several investigators. Although the geometrical configurations used differ from the two parallel vertical walls assumed in §2, it is possible to make order-of-magnitude comparisons to test the extent to which the wetting edge condition accounts for the action of surface tension in the damping of the waves.

3.1. *Benjamin & Ursell (1954)*

In these experiments a circular container was oscillated vertically to produce the parametric excitation of a standing wave in the contained fluid. The frequency of the wave generated was found to be in good agreement with the predicted value, but the damping rate was found to be up to 20 times that calculated from viscous dissipation in the boundary layer on the wall. The authors state that the discrepancy may be due to their neglect of surface-tension effects. The details of their apparatus suggest that an appropriate comparison between their results and those calculated from the results obtained in §2 can be made by taking K to be about 0.2 and $f^{\frac{1}{2}}$ about 0.03. Results calculated for this value of K and for various values of λ are shown in table 3, where the first line contains the damping rate associated with surface tension and the second line contains the viscous effect. From these results it can be seen that it is possible for the surface-tension effect to be more than 10 times the viscous effect when λ is less than about 2, but that the ratio decreases as λ is increased, with the viscous effect becoming the dominant one for λ greater than 10.

It appears, therefore, that the proposed wetting edge condition can account for the excessive damping observed in the experiments. Some caution is necessary, however, in claiming that this is the true cause of the high damping rates. The authors do not state what precautions they took to avoid the presence of surfactant materials, which are known to alter the behaviour of surface waves to a marked extent.

3.2. *Case & Parkinson (1957)*

These experiments were performed in circular cylinders of two different radii filled to various levels. The fundamental sloshing mode was excited by rocking the cylinder. The measured frequencies were slightly higher than those predicted by ignoring surface tension and using the free-end edge condition. The authors attribute this discrepancy of about 5 % to capillary effects associated with wetting of the cylinder wall. The damping rate was also close to that predicted from viscous dissipation, the agreement being improved when the observed frequencies were used instead of the theoretical values. When the water depth was less than the radius of the cylinder the agreement was not so good, but here we consider only the deep water results.

The values of K and f appropriate to the experiments are given by $K = 0.017$, $f^{\frac{1}{2}} = 0.011$ for the cylinder of radius 38 mm, and $K = 0.0042$, $f^{\frac{1}{2}} = 0.0065$ for the cylinder of radius 76 mm. When allowance is made for the increased area of the cylinder walls compared with that of the two plane walls, the observations are in reasonable agreement with those in tables 1 and 2. For the smaller cylinder, surface tension dominates viscosity as the important damping mechanism when λ is less than 5 and the maximum ratio of the two contributions to the total damping rate is about 8 when $\lambda = 0.2$. For the larger cylinder, surface tension dominates when λ is less than 2 and the ratio has a maximum value of about 3, again when $\lambda = 0.2$.

λ	0.1	0.2	0.5	1	2	5	10	20	50	100
Capillary	0.0754	0.146	0.219	0.126	0.064	0.025	0.013	0.006	0.002	0.001
Viscous	0.0048	0.0062	0.0101	0.0078	0.0072	0.0071	0.0071	0.0071	0.0071	0.0071
Ratio	16	23	22	16	8.9	3.5	1.8	0.85	0.28	0.14

TABLE 3. Damping rates for $K = 0.2$ and $f^{\frac{1}{2}} = 0.03$

An interesting feature of these experiments was the variation in damping rates between unpolished and polished surfaces. When the cylinder surfaces were polished the measured damping rates agreed with the predictions based on viscous damping only and the free-end edge condition. In the unpolished state the damping rate reached values two or three times those for the polished surfaces. These results are consistent with those of §2 if we assume a value for λ greater than 10 for the polished, and about 1 for the unpolished cylinders. The presence of surface roughnesses in the unpolished state, if sufficiently large, would suggest that the pinned-end edge condition should apply, the static range of contact angles being large enough to suppress any motion of the contact line. However, there would then be no damping associated with surface tension and the remaining viscous contribution would be about one-half of that in the free-end case. The increased damping in the unpolished cylinders cannot be explained in this way. If the surface roughnesses before polishing were not large, it is arguable that the wetting edge condition with moderate values of λ is appropriate, and the results obtained are not inconsistent with this hypothesis.

3.3. *Keulegan (1959)*

The containers used in these experiments were similar rectangular tanks with a width/length ratio of 0.22 and a depth/length ratio of 0.43. Rocking of the container produced the fundamental sloshing mode, with a single nodal line half-way along the tank and no variation across its width. The measured dissipation was split into two parts, a viscous part and a part due to surface tension. The viscous part was found to be proportional to $\nu^{\frac{1}{2}}$, as expected; the second part was shown to be proportional to the surface tension. A change to containers made of lucite was accompanied by an increase in the damping, the surface tension component being about six times that when glass tanks were used.

It is difficult to make qualitative comparisons between these results for shallow and narrow tanks and the theory of §2 which relates more readily to deep and wide containers. In the parameterization used by Keulegan the width/length ratio enters to the third power. The presence of a surface tension component in the total damping points to some mechanism of the sort modelled by the wetting edge condition and the increased damping when lucite replaces glass is consistent with a change in the parameter λ. The capillary contribution to the damping rate is denoted as α_2 by Keulegan and is related to the quantities defined in §2 by the equation

$$\alpha_2 = \frac{\mathrm{Im}\,(\sigma_0)}{\mathrm{Re}\,(\sigma_0)}. \tag{41}$$

For the small values of K relevant to the experiments, the results in table 1 predict that α_2 should be proportional to K as found in the experiments. Since the distilled water used in the experiments wets glass easily, large values of λ are appropriate in this case. With containers made of lucite, which is not readily wetted by water, a

moderate value of λ should be used. For the small values of K relevant to the experiments the capillary damping can be increased by a factor of 10 by reducing λ from 10 to 1 or from 5 to 0.5. When increasing amounts of a wetting agent were added to the water in the lucite containers the damping rate decreased until it became comparable with that in the glass containers. This decrease is consistent with the value of λ being increased by the presence of the wetting agent.

In this paper, it has been shown how a theoretical determination of the damping of surface waves by capillary action can be made. This damping is associated with conditions at the line of contact between the fluid and the container. The size of the capillary component is such that it may make a significant contribution to the total damping rate, sometimes a dominant one. Since the wetting edge condition can account at least partially for the effect of surface tension in dissipating the wave energy, the next step is to obtain quantitative estimates of damping rates in cylindrical and rectangular containers of finite depth. These estimates would enable a more satisfactory comparison with the experimental results to be made. Another possible extension is to adapt the wetting edge condition to include contact-angle hysteresis. The contact line would then have a stick–slip motion; when the line reaches its extreme positions it remains stationary for a period during which the contact angle varies over the static range before reversing its motion. Another important extension would be to remove the restriction to contact angles close to 90°. This is of particular importance for the case of wetting fluids, when the contact angle may be very small, but it is not clear to me how this extension could easily be made.

REFERENCES

Benjamin, T. B. & Scott, J. C. 1979 *J. Fluid Mech.* **92**, 241.

Benjamin, T. B. & Ursell, F. 1954 *Proc. R. Soc. Lond.* A **225**, 505.

Case, K. M. & Parkinson, W. C. 1957 *J. Fluid Mech.* **2**, 172.

Davis, S. H. 1980 *J. Fluid Mech.* **98**, 225.

Dussan V., E. B. 1979 *Ann. Rev. Fluid Mech.* **11**, 371.

Graham-Eagle, J. 1983 *Math. Proc. Camb. Phil. Soc.* **94**, 553.

Graham-Eagle, J. 1984 Gravity–capillary waves with edge constraints. D.Phil. thesis. University of Oxford.

Jansons, K. M. 1985 *J. Fluid Mech.* **154**, 1.

Keulegan, G. H. 1959 *J. Fluid Mech.* **6**, 33.

Lamb, H. 1932 *Hydrodynamics* 6th edn. Cambridge University Press.

Mei, C. C. & Liu, L. F. 1973 *J. Fluid Mech.* **59**, 239.

Miles, J. W. 1967 *Proc. R. Soc. Lond.* A **297**, 459.

Ursell, F. 1952 *Proc. R. Soc. Lond.* A **214**, 79.